Pergamon

Computers Math. Applic. Vol. 35, No. 5, pp. 93–106, 1998

0898-1221/98 $19.00 + 0.00

PII: S0898-1221(98)00008-X

A Delay and Loss Versatile Scheduling Discipline in ATM Switches

JEN M. HAH AND MARIA C. YUANG
Department of Computer Science and Information Engineering
National Chiao Tung University, Taiwan, R.O.C.

(Received August 1996; revised and accepted April 1997)

Abstract—In this paper, we propose a versatile scheduling discipline, called *Precedence with Partial Push-out* (PPP), in Asynchronous Transfer Mode (ATM) switches supporting two delay and two loss priorities. By employing a threshold L, the PPP discipline provides delay guarantee by allowing a newly-arriving high-delay-priority cell to precede a maximum of L, low-delay-priority cells. Through the use of another threshold R, the discipline offers loss guarantee by permitting a newly-arriving high-loss-priority cell to push out the last low-loss-priority cell located beyond the R^{th} location in a full queue. By setting L and R properly, PPP versatilely performs as any one of the four widely-accepted disciplines, namely, the FCFS, head-of-line, push-out, or head-of-line with push-out disciplines. For precisely determining L and R retaining demanded Quality of Services (QoSs), we provide an in-depth queueing analysis for the Cell Delay (CD) and Cell Loss Ratio (CLR) of high-delay-priority, low-loss-priority cells. We further propose a simple, algebra-based analysis for the CD and CLR of low-delay-priority, high-loss-priority cells. On the basis of these analyses, L and R can be dynamically and effectively adjusted to provide adequate delay and loss guarantees for high-priority cells while incurring only minimal performance degradation for other classes of cells. Finally, the paper presents simulation results confirming the accuracy of the analyses.

Keywords—Asynchronous Transfer Mode (ATM), Quality of Services (QoSs), Scheduling discipline, Push-out, Cell Delay (CD), Cell Loss Ratio (CLR).

1. INTRODUCTION

Asynchronous Transfer Mode (ATM) [1,2] has been widely accepted as a key technology for supporting a variety of traffic classes in Broadband-ISDNs [3]. To fully utilize limited network resources while providing satisfactory Quality of Services (QoSs) for network users, ATM switches are required to employ viable scheduling disciplines to mediate ATM cells departure and discard on a priority basis. These priority-based scheduling disciplines basically fall into one of three main categories: delay-based [4–7], loss-based [8–11], or delay-and-loss-based [8,10,11].

In the delay-based category, the Head-Of-the-Line (HOL) discipline [4] successfully offers stringent delay guarantee for real-time cells but at the expense of an increase in buffering delay for nonreal-time cells. Afterwards, a number of disciplines attempt to explicitly control the performance tradeoff between real-time and nonreal-time cells. Among them, the Minimum Laxity Threshold (MLT) [5] and Earliest Due Date (EDD) disciplines [6] manage the performance tradeoff from the *time* perspective. The MLT discipline grants higher priority to real-time cells only when the minimum laxity (defined as the amount of time until the earliest deadline of a queued real-time cell expires) is not over a threshold L. The EDD discipline allows a real-time cell to precede nonreal-time cells arriving not prior to D slot time. Rather than use the time perspective, the Queue Length Threshold (QLT) [5] and Threshold Based Priority (TBP) disciplines [7] manage

the performance trade-off from the *space* perspective. The QLT discipline concedes precedence to real-time cells only when the number of queued nonreal-time cells is not over a threshold T. The TBP discipline, on the other hand, agrees real-time cells to take precedence when the number of queued real-time cells exceeds a threshold L. All of these four disciplines successfully retain adequate QoSs for real-time cells while offering the best possible service to nonreal-time cells. Essentially, the success of these disciplines hinges on the effective determination of the threshold (L, D, or T).

In the loss-based category, the Complete Buffer Partitioning discipline [8] divides the queue into two regions dedicated to loss-sensitive and loss-insensitive cells, respectively. This discipline is prone to queue wastage since no queue sharing takes place. The Nested Threshold Cell Discarding (NTCD) (also referred to as partial buffer sharing) discipline [8–11] allows loss-insensitive cells to share the queue until the queue occupancy has reached a threshold T. The NTCD discipline results in poor space utilization should the load of loss-sensitive traffic be low. To alleviate the problem, the Push-Out buffer sharing (PO) discipline [8–11] further allows newly-arriving loss-sensitive cells to push out loss-insensitive cells if the queue is full. However, the PO discipline does not offer any adjustment of the Cell Loss Ratio (CLR) for any traffic class. This has motivated the deployment of the Threshold Push-Out (TPO) and P_{ow} Push-Out (P_{ow}PO) disciplines [9]. In the TPO discipline, a loss-sensitive cell observing a full queue upon its arrival can push out a loss-insensitive cell if the number of loss-insensitive cells exceeds a threshold T. In the P_{ow}PO discipline, a newly-arriving loss-sensitive cell observing a full queue can push out a loss-insensitive cell with probability P_{ow}. Again, the determination of T and P_{ow} has been essential and nontrivial.

To consider both delay and loss requirement, in the delay-and-loss-based category, the Nested Threshold Cell Discarding with Multiple Buffers (NTCD-MB) discipline [10] allows real-time cells to enter one smaller-size queue employing NTCD and grants loss-sensitive cells to enter the other larger-size queue. Loss-sensitive cells are served only when there is no real-time cell in the smaller-size queue. It offers stringent delay and loss guarantees for real-time cells and loss-sensitive cells, respectively. Nevertheless, this discipline causes poor space utilization due to the employment of two independent queues. The Head-of-the-Line with Push-Out (HLPO) discipline [8,11] uses HOL and PO disciplines for real-time cells and loss-sensitive cells, respectively. However, the HLPO discipline does not provide any adjustment of the Cell Delay (CD) and CLR for any traffic class.

In this paper, we propose a versatile scheduling discipline, called *Precedence with Partial Push-Out* (PPP), for ATM switches supporting two delay and two loss priorities. By employing a threshold L, the PPP discipline provides delay guarantee by allowing a newly-arriving high-delay-priority cell to precede a maximum of L low-delay-priority cells in a nonfull queue. Through the use of another threshold R, the discipline offers loss guarantee by permitting a newly-arriving high-loss-priority cell to push out the last low-loss-priority cell located beyond the R^{th} location in a full queue. By setting L and R differently, PPP can versatilely perform as any one of the following disciplines previously described, namely, the FCFS, HOL, PO, or HLPO discipline.

For precisely determining L and R retaining demanded QoSs, the paper provides an in-depth queueing analysis for the CD and CLR of high-delay-priority, low-loss-priority cells based on a discrete-time single-server queueing model with two heterogeneous arrivals. These arrivals are represented by Bernoulli processes and Interrupted Bernoulli Processes (IBPs). As for the CD and CLR of low-delay-priority, high-loss-priority cells, a simple, algebra-based analysis is employed. On the basis of the these analyses, L and R can be dynamically and effectively adjusted to provide adequate delay and loss guarantees for high-priority cells while incurring only minimal performance degradation for cells of other classes. Finally, the paper presents simulation results confirming the accuracy of these analyses.

The rest of the paper is organized as follows. Section 2 describes the PPP discipline in detail. The models and analyses for the CD and CLR of each traffic class is presented in Section 3.

Section 4 demonstrates the analytic and simulation results under a variety of traffic conditions and system constraints. Finally, Section 5 concludes the paper.

2. PPP SCHEDULING DISCIPLINE

Generally, PPP allows a newly-arriving high-delay-priority cell to precede a maximum of L low-delay-priority cells in a nonfull queue. Moreover, it grants a newly-arriving high-loss-priority cell to push out the last low-loss-priority cell located beyond the R^{th} location in a full queue. For convenience, ranges $[1, R]$ and $[R+1, K]$ of the queue of size K is referred to as the *safe region* and the *push-out region*, respectively. The detailed PPP discipline is formally described in Figure 1. Notice that FCFS, HOL, PO, and HLPO disciplines are all special cases of the PPP discipline. Specifically, PPP behaves as an FCFS discipline if L is set to zero and R is set to K, and performs as an HOL discipline if L and R are both set to K. Furthermore, PPP becomes a PO discipline if L and R are both set to zero, and acts as an HLPO discipline if L is set to K and R is set to zero.

- Queue newly-arriving cells based on the following criteria:
  If a cell observes a nonfull queue upon its arrival
    If the cell is high-delay-priority
      The cell precedes a maximum of L low-delay-priority cells;
    Else
      The cell is placed behind the last queued cell;
  Else
    If the cell is high-loss priority and there are low-loss-priority cells in the push-out region
      The cell pushes out the last low-loss-priority cell in the push-out region;
    Else
      The cell is discarded;
  If multiple cells arrive
    The high-delay-priority cells take precedence in entering the queue;
  If multiple cells of the same priority arrive
    These cells enter the queue in a random manner.
- Serve cells sequentially.

Figure 1. PPP scheduling discipline.

An example of how PPP operates under $L = 3$, $R = 6$, and $K = 10$ is illustrated in Figure 2. The number x^y, tagged in each cell denotes the x^{th}-arriving cell in Class-y, where $y = 0$ denotes the class of high delay-priority and high loss-priority, $y = 1$ denotes the class of high delay-priority and low loss-priority, $y = 2$ denotes the class of low delay-priority and high loss-priority, and finally, $y = 3$ denotes the class of low delay-priority and low loss-priority. As shown in the figure, in the first slot time (where slots are fixed in length), high-delay-priority cells 1^0 and 1^1 queue before simultaneously-arriving low-delay-priority cells $1^3, 1^2, 2^2$, and 2^3. In the second slot time, high-delay-priority cells $2^1, 2^0$, and 3^1 precede three low-delay-priority cells $1^2, 2^2$, and 2^3 since L is set to 3. In the third slot time, the queue is full after high-delay-priority cell 4^1 enters. Sequentially, high-loss-priority cells 5^2 and 6^2 push out low-loss-priority cells 4^1 and 3^3 from the push-out region, respectively. Moreover, high-loss-priority cell 7^2 is discarded since there is no low-loss-priority cell in the push-out region. Low-loss-priority cell 4^3 is also discarded since the queue is full.

3. QUEUEING MODEL AND ANALYSIS

Any nonbursty source stream (such as files, or any stream output from a traffic shaper [12]) is modelled as a Bernoulli process (called the M-stream), whereas any bursty source stream (such

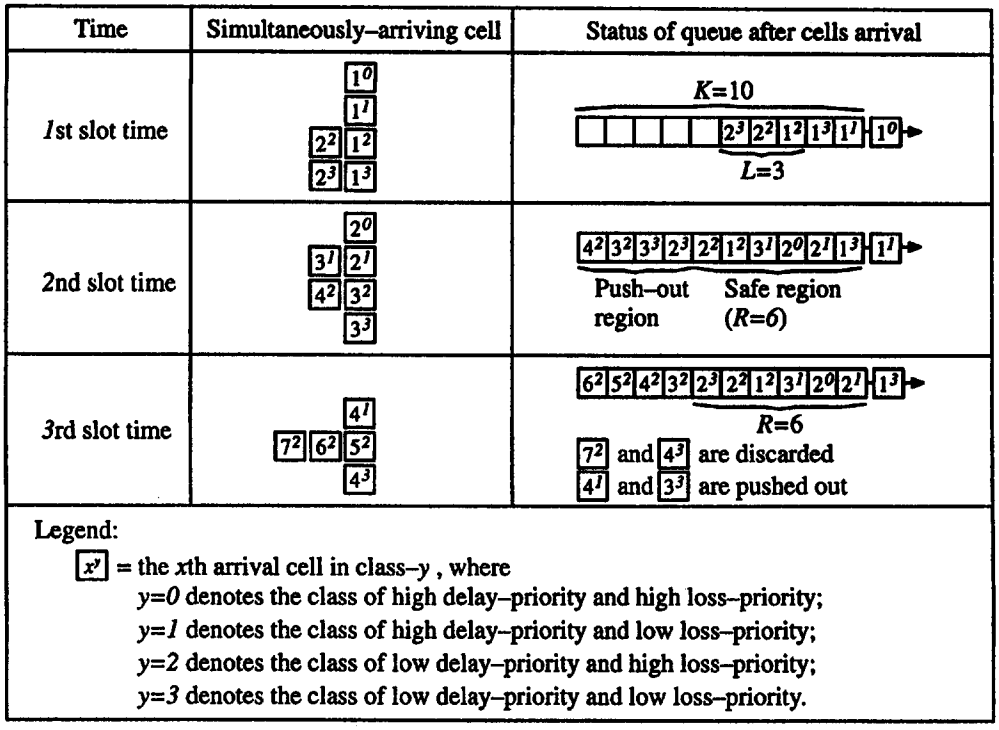

Figure 2. The PPP discipline ($L = 3$, $R = 6$, and $K = 10$)—an example.

as voice, or video) is modeled as an IBP (called the I-stream) [13,14]. For M-streams, let N_M be the number of M-streams and R_M be the mean cell arrival rate (cells/slot time) for each M-stream. The probability mass function (pmf) of the number of M-cells arriving in a slot time, denoted as $m(j)$, follows a binomial distribution, namely, $m(j) = \binom{N_M}{j} \cdot R_M^j \cdot (1 - R_M)^{N_M - j}$.

For I-streams, let N_I be the number of I-streams. In one slot time, an I-stream changes from state ON to OFF with probability $1 - \alpha$ and from state OFF to ON with probability $1 - \beta$ per slot, respectively. An I-stream generates a cell by a rate of λ in the ON state and generates no cell in the OFF state. The pmf of the number of I-cells arriving in a slot time given i I-streams in the ON state, denoted as $b_i(j)$, follows a binomial distribution, namely, $b_i(j) = \binom{i}{j} \cdot \lambda^j \cdot (1-\lambda)^{i-j}$, and the transition probability $p_{h,i}$, that the number of I-streams in the ON state changes from h to i can be obtained as $p_{h,i} = \sum_{x=0}^{h} \binom{h}{x} \alpha^x (1-\alpha)^{h-x} \binom{N_I - h}{i-x} (1-\beta)^{i-x} \beta^{N_I - h - (i-x)}$. Without loss of generality, I-streams and M-streams can also be categorized as the high-delay-priority, low-loss-priority class and the low-delay-priority, high-loss-priority class, respectively, in the paper.

Moreover, each ATM switch is assumed to employ the output buffering mechanism and the PPP discipline. Each output buffer (buffer size = K) of a switch thus becomes the $M^{[N_M]} + I^{[N_I]}/D/1/K$ with PPP system. During system operation, at the beginning of each slot time, four simultaneous events occur. They are the following.

Event (1): the number of I-streams in the ON state changes.
Event (2): I-cells arrive.
Event (3): M-cells arrive. At the end of each slot time, Event (4) occurs.
Event (4): the cell in the server departs.

In the following, the system occupancy distribution is derived first. Based on the system occupancy distribution, we then compute two performance metrics (the CD and CLR) which serve as the foundation of the determination of L and R.

3.1. System Occupancy Distribution

The system occupancy distribution is observed at each slot time, where the system means the server and the queue. As shown in Figure 3, $\tilde{X}$ and $\tilde{Y}$ denote the number of queued cells which

cannot be and can be preceded by newly-arriving I-cells, respectively. That is, the number of cells in the system is divided into $\tilde{X}$ and $\tilde{Y}$. Denote $\tilde{I}$ as the number of I-streams in the ON state. Thus, the system occupancy distribution is defined as the pmf of $\tilde{X}, \tilde{Y}$, and $\tilde{I}$, denoted as $f(j,l,i)$.

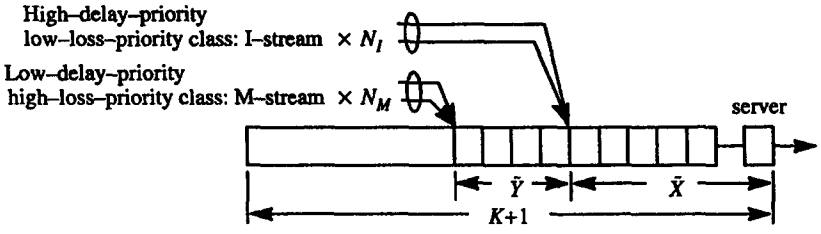

Figure 3. Analytic model.

Let $f^{(n)}(j,l,i)$ and $\overline{f^{(n)}}(j,l,i)$ be the system occupancy distribution observed at the n^{th} slot time after the occurrence of Events (1) and (4), respectively. After the occurrence of Event (1), $\tilde{X}$ and $\tilde{Y}$ both are not changed. Hence, $f^{(n)}(j,l,i)$ is related to $\overline{f^{(n-1)}}(j,l,h)$, $0 \le h \le N_I$, by

$$f^{(n)}(j,l,i) = \sum_{h=0}^{N_I} \left(p_{h,i} \cdot \overline{f^{(n-1)}}(j,l,h) \right), \qquad 0 \le j \le K, \quad 0 \le l \le L, \quad 0 \le i \le N_I, \tag{1}$$

where $p_{h,i}$ is the transition probability defined in the previous subsection.

After the occurrence of Event (2), since newly-arriving I-cells can precede $\tilde{Y}$ M-cells, these I-cells are placed behind the $\tilde{X}^{\text{th}}$ queued cell. Thus, $\tilde{X}$ is increased by the number of these I-cells but only up to $K+1-\tilde{Y}$ where $K+1$ is the maximum number of cells in the system. Owing to the pmf of the sum of two independent random variables is the convolution of the individual pmf, the system occupancy distribution observed at the n^{th} slot time after the occurrence of Event (2), $\vec{f^{(n)}}(j,l,i)$, can be obtained by

$$\vec{f^{(n)}}(j,l,i) = \min_X \left(f^{(n)}(j,l,i) \oplus b_i(j) \right), \qquad 0 \le j \le K+1, \quad 0 \le l \le L, \quad 0 \le i \le N_I, \tag{2}$$

where $\oplus$ is the convolution operator, and $\min_X$ is the function defined as

$$\min_X (g(j,l,i)) = \begin{cases} g(j,l,i), & j < K+1-l, \\ \sum_{h=K+1-l}^{\infty} g(h,l,i), & j = K+1-l, \\ 0, & \text{otherwise.} \end{cases} \tag{3}$$

After the occurrence of Event (3), newly-arriving M-cells are placed behind the last queued cell. Therefore, $\tilde{Y}$ is increased by the number of these M-cells, but only up to L and $\tilde{X}$ has to be readjusted as well since L is the maximum number of M-cells which can be preceded by I-cells. In this case, $\tilde{X}$ is increased by the exceeding value of $\tilde{Y}$ from L but only up to $K+1-\tilde{Y}$. Moreover, owing to the nonpreemptive property of the server, the M-cell in the server will not be preceded by the next-arriving I-cell. Thus, $\tilde{X}$ is increased by 1 and $\tilde{Y}$ is decreased by 1 if there are only M-cells in the system, namely, $\tilde{X} = 0$ and $\tilde{Y} > 0$. The system occupancy distribution observed at the n^{th} slot time after the occurrence of Event (3), $\overleftrightarrow{f^{(n)}}(j,l,i)$ can be given as

$$\overleftrightarrow{f^{(n)}}(j,l,i) = \begin{cases} \min_X \left(\min_Y \left(\vec{f^{(n)}}(1,l,i) \oplus m(l) \right) \right) & \\ \quad + \min_X \left(\min_Y \left(\vec{f^{(n)}}(0,l+1,i) \oplus m(l+1) \right) \right), & j = 1, \ 0 \le l < L, \\ 0, & j = 0, \ 1 \le l \le L, \\ \min_X \left(\min_Y \left(\vec{f_i^{(n)}}(j,l,i) \oplus m(l) \right) \right), & \text{otherwise,} \end{cases} \tag{4}$$

where $\min_Y$ is the function defined as

$$\min_Y (g(j,l,i)) = \begin{cases} g(j,l,i), & l < L, \\ \sum_{h=0}^{\infty} g(j-h, l+h, i), & l = L, \\ 0, & \text{otherwise.} \end{cases} \tag{5}$$

After the occurrence of Event (4), each cell shifts ahead one system location. Hence, $\tilde{X}$ is decreased by 1 but only down to 0. Again, on account of the nonpreemptive property of the server, the M-cell in the server will not be preceded by the next-arriving I-cell. Accordingly, $\overline{f^{(n)}}(j,l,i)$ becomes

$$\overline{f^{(n)}}(j,l,i) = \begin{cases} \max\left(\overleftrightarrow{f^{(n)}}(1,l,i)\right) + \max\left(\overleftrightarrow{f^{(n)}}(0,l,+1,i)\right), & j = 1,\ 0 \le l \le L, \\ 0, & j = 0,\ 1 \le l \le L, \\ \max\left(\overleftrightarrow{f^{(n)}}(j,l,i)\right), & \text{otherwise,} \end{cases} \tag{6}$$

where max is the function defined as

$$\max(g(j,l,i)) = \begin{cases} g(0,l,i) + g(1,l,i), & j = 0, \\ g(j+1,l,i), & 1 \le j \le K-l, \\ 0, & \text{otherwise.} \end{cases} \tag{7}$$

As a result, from equations (1), (2), (4), and (6), we can obtain $f(j,l,i)$ by

$$f(j,l,i) = \lim_{n\to\infty} f^{(n)}(j,l,i), \qquad 0 \le j \le K, \quad 0 \le l \le L, \quad 0 \le i \le N_I, \tag{8}$$

with initial condition $\sum_{i=0}^{N_I}\sum_{l=0}^{L}\sum_{j=0}^{K}\overline{f^{(0)}}(j,l,i) = 1$.

3.2. CD and CLR for I-cells

We are now at the stage of computing the system time distribution CD and CLR for I-cells based on the previously derived system occupancy distribution $f(j,l,i)$. Let $\tilde{Z}$ denote the system location in which the observed I-cell (called the I^0-cell) is placed upon its arrival. Notice that $\tilde{Z}$ is a metric for determining if the I^0-cell would be pushed out at later time. $\tilde{Z}$ is the sum of (1), the order by which the I^0-cell is served among simultaneously-arriving cells, and (2), the number of queued cells which cannot be presented by the I^0-cell. Thus, we are to find the pmf of the first term given i I-streams in the ON state, denoted by $r_i(j)$. Moreover, the pmf of the second term can be indirectly obtained from the system occupancy distribution observed by I-cells, denoted by $\hat{f}(j,l,i)$.

To derive $r_i(j)$, let $\tilde{B}_{i,\bar{0}}$ denote the positive number of I-cells arriving in a slot time given i I-streams in the ON state, and $b_{i,\bar{0}}(h)$ be its pmf. $b_{i,\bar{0}}(h)$ is given as $b_{i,\bar{0}}(h) = b_i(h)/(1-b_i(0))$. Moreover, let $\tilde{\tilde{B}}_{i,\bar{0}}$ denote the positive number of I-cells including the I^0-cell arriving in a slot time given i I-streams in the ON state, and $\hat{b}_{i,\bar{0}}(h)$ be its pmf. From renewal theory [4], $\hat{b}_{i,\bar{0}}(h)$ is obtained as $\hat{b}_{i,\bar{0}}(h) = h \cdot b_{i,\bar{0}}(h)/E[\tilde{B}_{i,\bar{0}}]$, where E is the mean function. Accordingly, $r_i(j)$ becomes

$$r_i(j) = \sum_{h=j}^{N_I} \frac{\hat{b}_{i,\bar{0}}(h)}{h}, \qquad 1 \le j \le N_I, \quad 0 \le i \le N_I, \tag{9}$$

where $1/h$ is the probability that the I^0-cell is served, the j^{th} among h I-cells.

To derive $\hat{f}(j,l,i)$ on the basis of $f(j,l,i)$, let $\tilde{I}_{\bar{0}}$ be the positive number of I-streams in the ON state, and $\phi_{\bar{0}}(i)$ be its pmf. $\phi_{\bar{0}}(i)$ is expressed as $\phi_{\bar{0}}(i) = \phi(i)/(1-\phi(0))$, where $\phi(i)$ is the

probability of i I-streams in the ON state. Further, let $\tilde{\tilde{I}}_{\bar{0}}$ be the positive number of I-streams including the source of the I^0-cell in the ON state, and $\hat{\phi}_{\bar{0}}(i)$ be its pmf. Again, from renewal theory, $\hat{\phi}_{\bar{0}}(i)$ is given as $\hat{\phi}_{\bar{0}}(i) = i \cdot \phi_{\bar{0}}(i)/E[\tilde{I}_{\bar{0}}]$. Note, that $\hat{f}(j,l,i)$ is observed upon arrivals of I-cells, and $f(j,l,i)$ is observed at each slot time. That is, $\sum_{l=0}^{L}\sum_{j=0}^{K}\hat{f}(j,l,i) = \hat{\phi}_{\bar{0}}(i)$ and $\sum_{l=0}^{L}\sum_{j=0}^{K} f(j,l,i) = \phi(i)$. Owing to the fact, under $\tilde{X} = a$, $\tilde{Y} = b$, and $\tilde{I} = c$, the ratio of $\hat{f}(a,b,c)$ to $f(a,b,c)$ is equal to $\hat{\phi}_{\bar{0}}(c)/\phi(c)$, $\hat{f}(j,l,i)$ becomes

$$\hat{f}(j,l,i) = f(j,l,i) \cdot \frac{\hat{\phi}_{\bar{0}}(i)}{\phi_i}, \qquad 0 \le j \le K, \quad 0 \le l \le L, \quad 0 \le i \le N_I. \tag{10}$$

Based on $r_i(j)$ and $\hat{f}(j,l,i)$, we now derive the system time distribution for I-cells, denoted as $s_I(j)$. According to the system location $\tilde{Z}$, $s_I(j)$ can be examined from three different conditions:

(i) the I^0-cell is in the safe region or the server upon its arrival,
(ii) the I^0-cell observes a full queue upon its arrival, and
(iii) the I^0-cell is in the push-out region.

CASE (i). Under the first condition, namely, $1 \le \tilde{Z} \le R+1$, the system time for the I^0-cell is equal to $\tilde{Z}$. From equations (9),(10), the system time distribution $s_I(j)$, $1 \le j \le R+1$, can be simply given as

$$s_I(j) = \sum_{i=0}^{N_I}\sum_{l=0}^{L}\left(\hat{f}(j,l,i) \oplus r_i(j)\right), \qquad 1 \le j \le R+1. \tag{11}$$

CASE (ii). For the second condition, namely $\tilde{Z} > K+1-\tilde{Y}$, the system time for the I^0-cell is not considered due to being discarded from the system. On the basis of equations (9),(10), the CLR for the I^0-cell, $\vec{L}_I$ is acquired as

$$\vec{L}_I = \sum_{i=0}^{N_I}\sum_{l=0}^{L}\sum_{j>K+1-l}^{\infty}\left(\hat{f}(j,l,i) \oplus r_i(j)\right). \tag{12}$$

CASE (iii). Under the third condition, namely $R+2 \le \tilde{Z} \le K+1-\tilde{Y}$, the I^0-cell may be pushed out before shifting into the safe region. We now discuss the push-out effect on the system time for the I^0-cell in the following context. Define $\tilde{V}$ as the number of M-cells queued behind the I^0-cell. Let $u^{(n)}(j,l,i)$ denote the probability that the I^0-cell is still in the push-out region where $\tilde{Z} = j$, $\tilde{V} = l$, and $\tilde{I} = i$, which is observed prior to the occurrence of Event (3) at the n^{th} slot time after the I^0-cell has arrived. Apparently n falls between 0 and $K-R-1$ since the push-out region is from $R+2$ to $K+1$. From equations (9),(10), $u^{(0)}(j,l,i)$ becomes

$$u^{(0)}(j,l,i) = \begin{cases} \hat{f}(j,l,i) \oplus r_i(j), & 0 \le l \le L,\ R+2 \le j \le K+1-l,\ 0 \le i \le N_I, \\ 0, & \text{otherwise.} \end{cases} \tag{13}$$

After the occurrence of Event (3) at the n^{th} slot time after the I^0-cell has arrived, newly-arriving M-cells are placed behind the last queued cell. Thus, $\tilde{V}$ is increased by the number of these M-cells. The I^0-cell is pushed out if $\tilde{V}$ is larger than the maximum number of M-cells queued behind the I^0-cell, namely $\tilde{V} > K+1-\tilde{Z}+n$. After the occurrence of Event (4) at the n^{th} slot time, since the I^0-cell shifts ahead one system location each slot time, the I^0-cell shifts into the safe region if the I^0-cell is placed at the $(R+2+n)^{\text{th}}$ system location upon its arrival, namely $\tilde{Z} = R+2+n$. Therefore, prior to the occurrence of Event (3) at the $(n+1)^{\text{th}}$ slot time, the I^0-cell still stays in the push-out region if the I^0-cell does not push out and does not shift into

the safe region, namely, $0 \le \tilde{V} \le K+1-\tilde{Z}+n$ and $R+2+n < \tilde{Z} \le K+1$. Accordingly, $u^{(n+1)}(j,l,i)$ is related to $u^{(n)}(j,l,i)$ by

$$u^{(n+1)}(j,l,i) = \begin{cases} u^{(n)}(j,l,i) \oplus m(l), & 0 \le n \le K-R-2,\ R+2+n < j \le K+1, \\ & 0 \le l \le K+1-j+n,\ 0 \le i \le N_I, \\ 0, & \text{otherwise.} \end{cases} \tag{14}$$

Moreover, the CLR for the I^0-cell at the n^{th} slot time, $\overleftrightarrow{L_I^{(n)}}$ is acquired as

$$\overleftrightarrow{L_I^{(n)}} = \sum_{i=0}^{N_I} \sum_{j=R+2+n}^{K+1} \sum_{l>K+1-j+n}^{\infty} \left(u^{(n)}(j,l,i) \oplus m(l)\right), \qquad 0 \le n \le K-R-1, \tag{15}$$

and the system time distribution $s_I(j)$, $j = R+2+n$ is obtained as

$$s_I(j) = \sum_{i=0}^{N_I} \sum_{l=0}^{K+1-j+n} \left(u^{(n)}(j,l,i) \oplus (m(l))\right), \qquad 0 \le n \le K-R-1, \quad j = R+2+n. \tag{16}$$

As a result, on the basis of equations (12) and (15), the CLR for I-cells (L_I) is given as

$$L_I = \vec{L}_I + \sum_{n=0}^{K-R-1} \overleftrightarrow{L_I^{(n)}}, \tag{17}$$

and from equations (11), (16), and (17), the CD for I-cells (D_I) can be simply expressed as

$$D_I = \sum_{j=1}^{K+1} \frac{j \cdot s_I(j)}{(1-L_I)}. \tag{18}$$

3.3. CD and CLR for M-cells

For deriving the CD and CLR for M-cells (denoted as D_M and L_M), we adopt a simple algebra-based analysis. Let $\hat{D}_M$ and $\hat{L}_M$ ($\hat{D}_I$ and $\hat{L}_I$) be the CD and CLR for M-cells (I-cells) which are derived based on the FCFS discipline, respectively. These metrics ($\hat{D}_M, \hat{L}_M, \hat{D}_I$, and $\hat{L}_I$) have been previously given by the same authors in [15]. Ultimately, D_M and L_M will be indirectly inferred from $D_I, L_I, \hat{D}_M, \hat{L}_M, \hat{D}_I$, and $\hat{L}_I$. Variables used throughout the algebraic analysis are summarized in Table 1.

Table 1. Variables used throughout the algebraic analysis.

Variable	Definition
$D_M, L_M (D_I, L_I)$	CD, CLR of M-cells (I-cells)
$\hat{D}_M, \hat{L}_M \left(\hat{D}_I, \hat{L}_I\right)$	CD, CLR of M-cells (I-cells) based on FCFS
$\mathcal{C}_M (\mathcal{C}_I)$	Total number of M-cells (I-cells) which have been discarded
$\hat{\mathcal{C}}_M \left(\hat{\mathcal{C}}_I\right)$	Total number of M-cells (I-cells) which have been discarded based on FCFS
$\mathcal{A}_M (\mathcal{A}_I)$	Total number of M-cells (I-cells) which have arrived
F	Ratio of $\mathcal{A}_M$ to $\mathcal{A}_I$
$N_M (N_I)$	Number of M-streams (I-streams)
$R_M (R_I)$	Mean cell arrival rate of an M-stream (I-stream)
$\mathcal{F}_M (\mathcal{F}_I)$	Total sojourn time of M-cell (I-cells) which have departed
$\hat{\mathcal{F}}_M \left(\hat{\mathcal{F}}_I\right)$	Total sojourn time of M-cells (I-cells) which have departed based on FCFS
$\mathcal{E}_M (\mathcal{E}_I)$	Total number of M-cells (I-cells) which have departed
$\overleftrightarrow{D_I}$	Mean sojourn time of pushed-out I-cells
$\overleftrightarrow{\mathcal{F}_I}$	Total sojourn time of pushed-out I-cells

To derive L_M, relate L_M, L_I, and F by

$$L_M = \frac{C_M}{\mathcal{A}_M}, \quad L_I = \frac{C_I}{\mathcal{A}_I}, \qquad \text{and} \quad F = \frac{\mathcal{A}_M}{\mathcal{A}_I} = \frac{N_M \cdot R_M}{N_I \cdot R_I}. \tag{19}$$

Therefore, we get

$$C_M + C_I = \mathcal{A}_M \cdot L_M + \mathcal{A}_I \cdot L_I = \mathcal{A}_I \cdot (F \cdot L_M + L_I), \qquad \text{and} \tag{20}$$

$$\hat{C}_M + \hat{C}_I = \mathcal{A}_M \cdot \hat{L}_M + \mathcal{A}_I \cdot \hat{L}_I = \mathcal{A}_I \cdot \left(F \cdot \hat{L}_M + \hat{L}_I\right), \tag{21}$$

Note, that at each slot time, the number of cells in the system based on PPP is identical to that based on FCFS. That is, the total number of cells which have been discarded based on PPP (i.e., $C_M + C_I$) is identical to that based on FCFS (i.e., $\hat{C}_M + \hat{C}_I$). Accordingly, on the basis of equations (20) and (21), L_M can be given as

$$L_M = \frac{F \cdot \hat{L}_M + \hat{L}_I - L_I}{F}. \tag{22}$$

To derive D_M, relate D_M, D_I, and $\overleftrightarrow{D}_I$ by

$$D_M = \frac{\mathcal{F}_M}{\mathcal{E}_M}, \quad D_I = \frac{\mathcal{F}_I}{\mathcal{E}_I}, \quad \text{and} \quad \overleftrightarrow{D}_I = \frac{\overleftrightarrow{\mathcal{F}}_I}{\mathcal{A}_I} = \sum_{n=0}^{K-R-1} \left(n \cdot \overleftrightarrow{L_I^{(n)}}\right), \tag{23}$$

where $\overleftrightarrow{L_I^{(n)}}$ is the probability that the sojourn time of a pushed-out I-cell is n slot time, and has been derived in equation (15). Moreover, from equation (19), $\mathcal{E}_M$ and $\mathcal{E}_I$ are expressed as

$$\begin{aligned} \mathcal{E}_M &= \mathcal{A}_M - \mathcal{C}_M = \mathcal{A}_M - \mathcal{A}_M \cdot L_M = \mathcal{A}_I \cdot F \cdot (1 - L_M), \qquad \text{and} \\ \mathcal{E}_I &= \mathcal{A}_I - \mathcal{C}_I = \mathcal{A}_I - \mathcal{A}_I \cdot L_I = \mathcal{A}_I \cdot (1 - L_I). \end{aligned} \tag{24}$$

Therefore, from equations (23) and (24), we get

$$\begin{aligned} \mathcal{F}_M + \mathcal{F}_I + \overleftrightarrow{\mathcal{F}}_I &= \mathcal{E}_M \cdot D_M + \mathcal{E}_I \cdot D_I + \mathcal{A}_I \cdot \overleftrightarrow{D}_I \\ &= \mathcal{A}_I \cdot \left(F \cdot (1 - L_M) \cdot D_M + (1 - L_I) \cdot D_I + \overleftrightarrow{D}_I\right), \qquad \text{and} \end{aligned} \tag{25}$$

$$\hat{\mathcal{F}}_M + \hat{\mathcal{F}}_I = \mathcal{A}_I \cdot \left(F \cdot \left(1 - \hat{L}_M\right) \cdot \hat{D}_M + \left(1 - \hat{L}_I\right) \cdot \hat{D}_I\right). \tag{26}$$

Moreover, since the sum of numbers of cells in the system observed at each slot time is identical to the total sojourn time of cells, the total sojourn time of cells based on PPP (i.e., $\mathcal{F}_M + \mathcal{F}_I + \overleftrightarrow{\mathcal{F}}_I$) is identical to that based on FCFS (i.e., $\hat{\mathcal{F}}_M + \hat{\mathcal{F}}_I$). Accordingly, on the basis of equations (25) and (26), D_M can be given as

$$D_M = \frac{F \cdot \left(1 - \hat{L}_M\right) \cdot \hat{D}_M + \left(1 - \hat{L}_I\right) \cdot \hat{D}_I - (1 - L_I) \cdot D_I - \overleftrightarrow{D}_I}{F \cdot (1 - L_M)}. \tag{27}$$

4. SIMULATION RESULTS

To verify the accuracy of analyses, we ran analytic results using MATLAB [16], and implemented the time-based simulation in the C language. The program for analytic computation terminated when all entries of matrix $|f^{(n)}(j,l,i) - f^{(n-1)}(j,l,i)|$ were dropped to 10^{-6} and below. The simulation program terminated when a loss of 10^4 cells was detected. Characteristics of traffic classes are summarized in Table 2. Figures 4–7 depict the CD and CLR of a switch with

traffic classes M and I. All these figures demonstrate profound agreement of analytic results with simulation results.

Figure 4 depicts the CD and CLR of each marked traffic class as functions of L under various Rs and a given set of N_M, N_I, and K. As shown in the figure, while CD is hardly affected by R, CLR is sensitive to R. In particular, the lower the R the lower the CLR of M-streams (and the higher the CLR of I-streams). This is because M-cells can push out more I-cells at lower R. In addition, the reduction effect of the CLR for M-streams becomes more significant as R decreases. Moreover, the CLR of M-streams has been greatly improved if L is less than the size of the push-out region, i.e., $L < K - R$. This is because, in this case, newly-arriving M-cells have greater possibility to push out an I-cell in the push-out region.

Table 2. Characteristics of traffic classes.

Traffic Class	Traffic Parameter	Delay QoS Requirement	Delay Priority	Loss QoS Requirement	Loss Priority
M	$R_M = 0.05$	60 slot time	low	1×10^{-6}	high
I	$\gamma = 5$; $\delta = 45$; $\lambda = 1.0$	15 slot time	high	5×10^{-3}	low

Legend:
R_M = mean cell arrival rate (cell/slot time) for an M-strea;
γ = mean ON length for an I-stream;
δ = mean OFF length for an I-stream;
λ = mean cell arrival rate for an I-stream in the ON state.

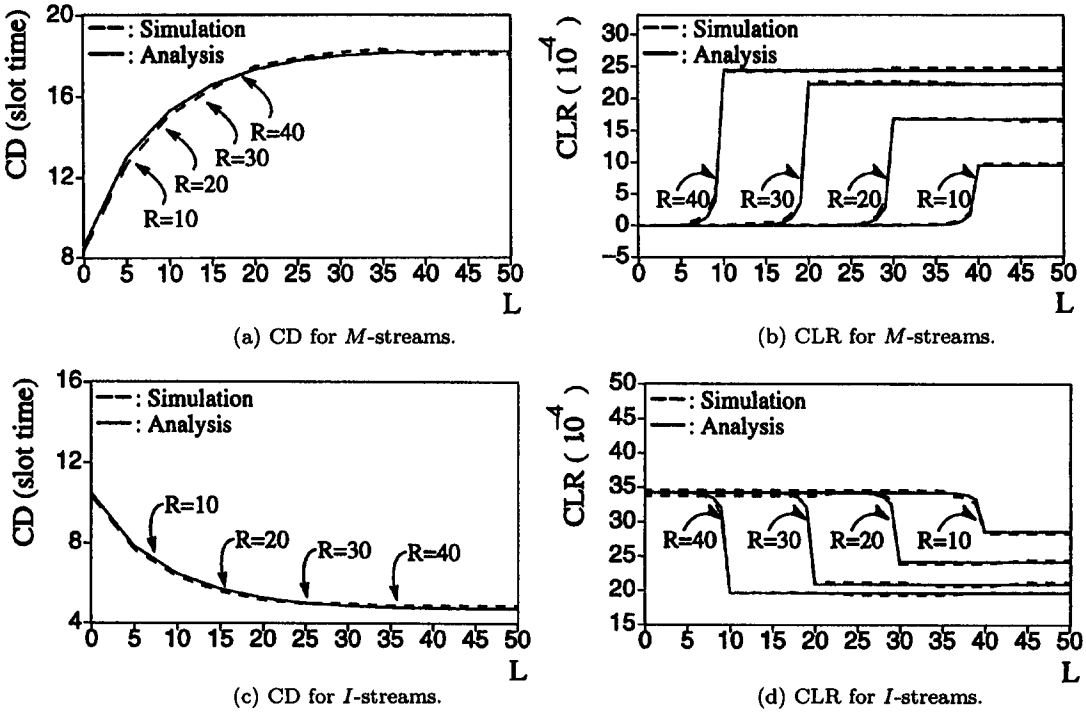

(a) CD for M-streams.

(b) CLR for M-streams.

(c) CD for I-streams.

(d) CLR for I-streams.

Figure 4. CD and CLR under various Rs ($N_M = 6$, $N_I = 5$, and $K = 50$).

Figure 5 exhibits the CD and CLR of each class as functions of L under various burstiness and a given set of N_M, N_I, R, and K. It is shown that the CD and CLR both increase with burstiness since an increase in burstiness results in a decrease in statistical multiplexing gain [17]. Furthermore, under the same mean cell arrival rate for an I-stream, the reduction effect of the CLR for M-streams (the CD for I-streams) becomes less (more) significant as the mean ON length of an I-stream decreases.

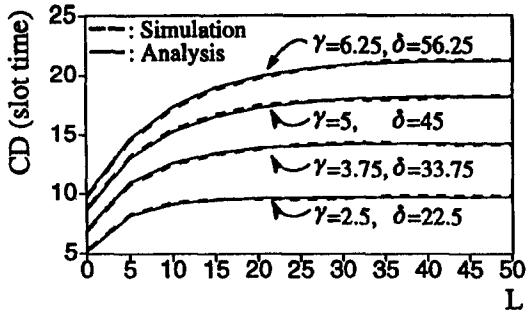

(a) CD for M-streams.

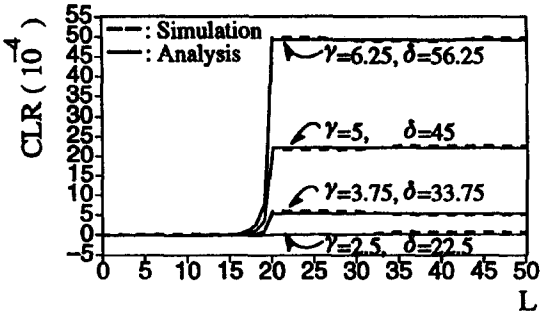

(b) CLR for M-streams.

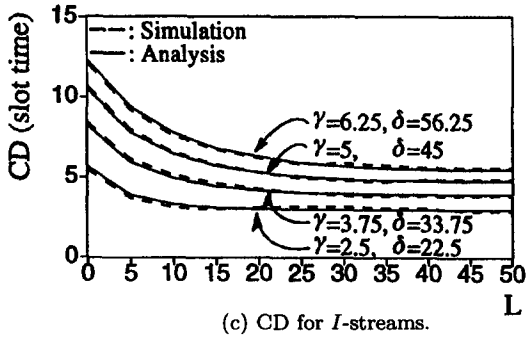

(c) CD for I-streams.

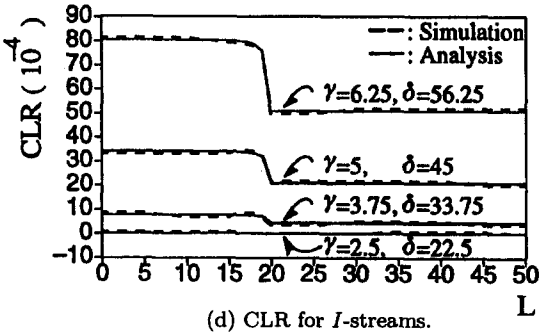

(d) CLR for I-streams.

Figure 5. CD and CLR under various burstiness ($N_M = 6$, $N_I = 5$, $R = 30$, and $K = 50$).

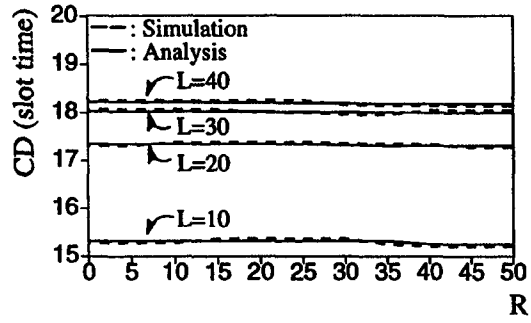

(a) CD for M-streams.

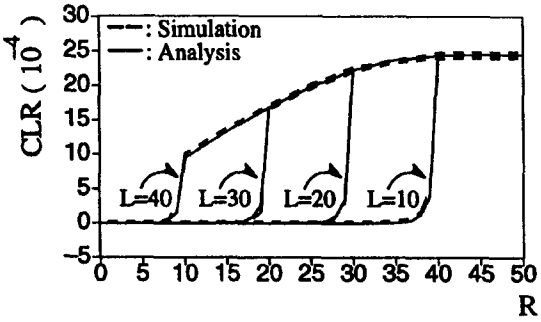

(b) CLR for M-streams.

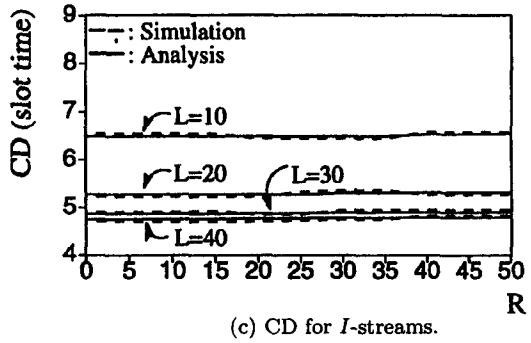

(c) CD for I-streams.

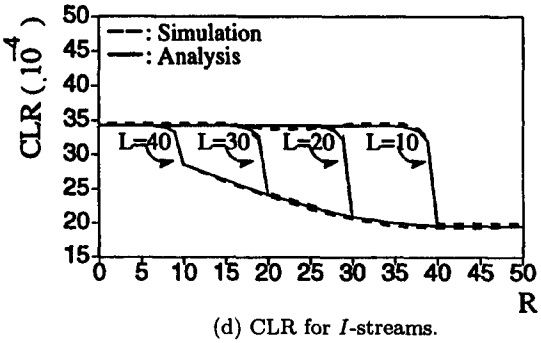

(d) CLR for I-streams.

Figure 6. CD and CLR under various Ls ($N_M = 6$, $N_I = 5$, and $K = 50$).

Figure 6 compares the CD and CLR of each traffic class as functions of R under various Ls and a given set of N_M, N_I, and K. This figure exhibits, that while CLR is almost unaffected by L, CD is sensitive to L. Especially, the CD is almost identical under the same L. Moreover, the greater the L, the lower the CD of I-streams (and the higher the CD of M-streams). The

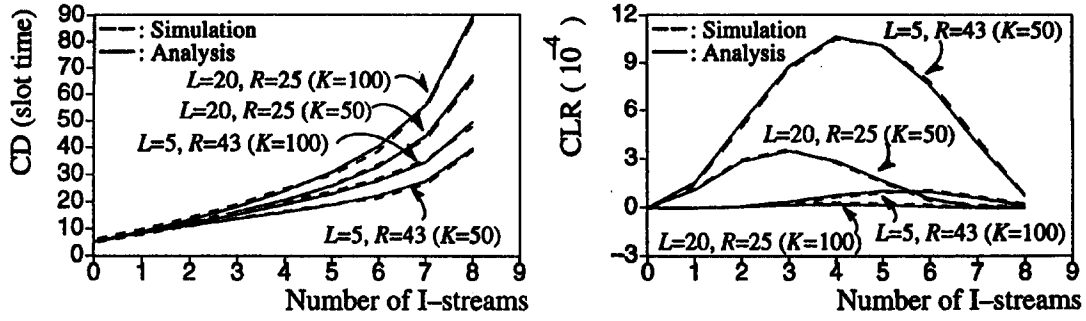

(a) CD for M-streams. (b) CLR for M-streams.

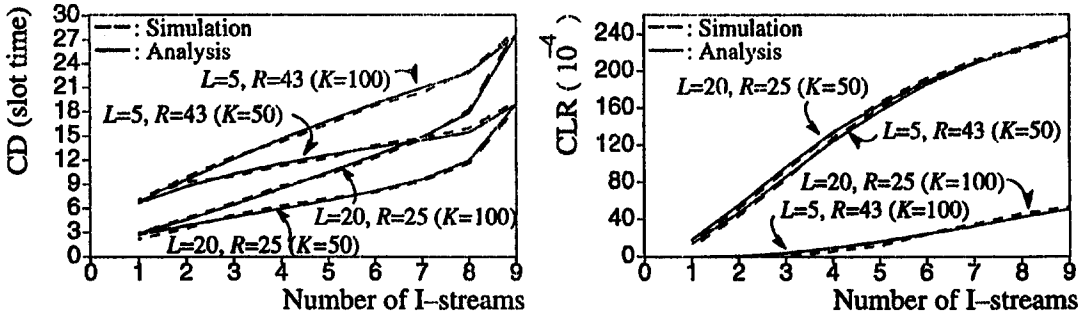

(c) CD for I-streams. (d) CLR for I-streams.

Figure 7. CD and CLR under different Ls and Rs ($\rho = 0.9$).

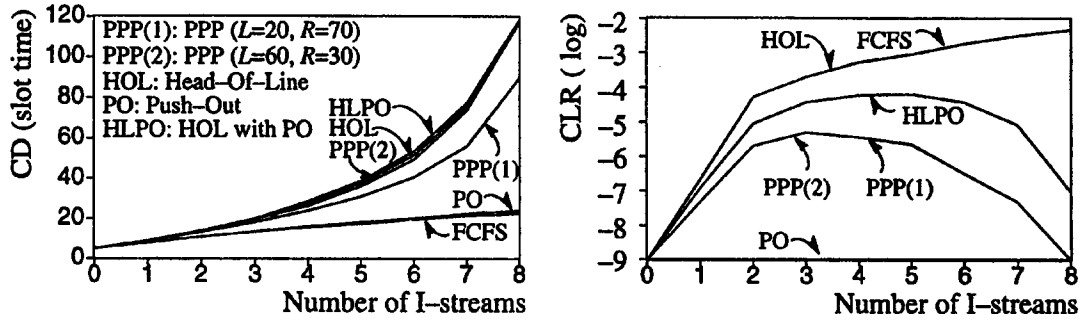

(a) CD for M-streams. (b) CLR for M-streams.

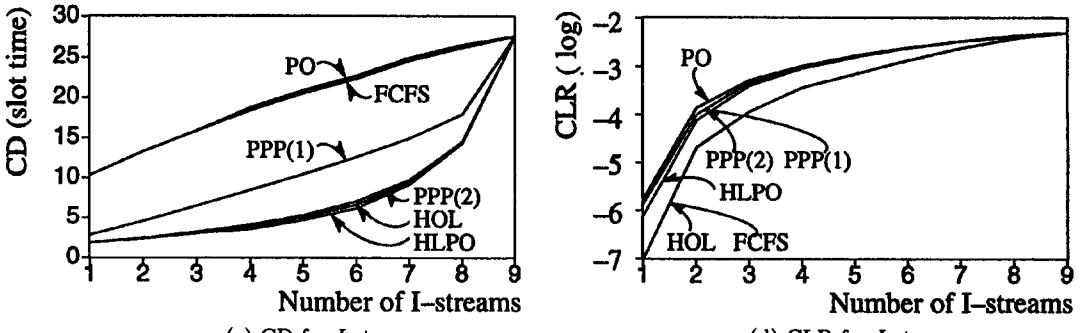

(c) CD for I-streams. (d) CLR for I-streams.

Figure 8. CD and CLR based on various disciplines ($\rho = 0.9$, $K = 100$).

rationale behind this fact is that I-cells can precede more M-cells with higher L. In addition, the reduction effect of the CD for I-streams becomes less significant as L increases.

Figure 7 shows the CD and CLR of each traffic class as functions of the number of I-streams under different Ls and Rs and a given set of ρ and K while retaining aggregate loads (ρ) of 0.9. The aggregate load is defined as the total traffic load of M-streams and I-streams. For example,

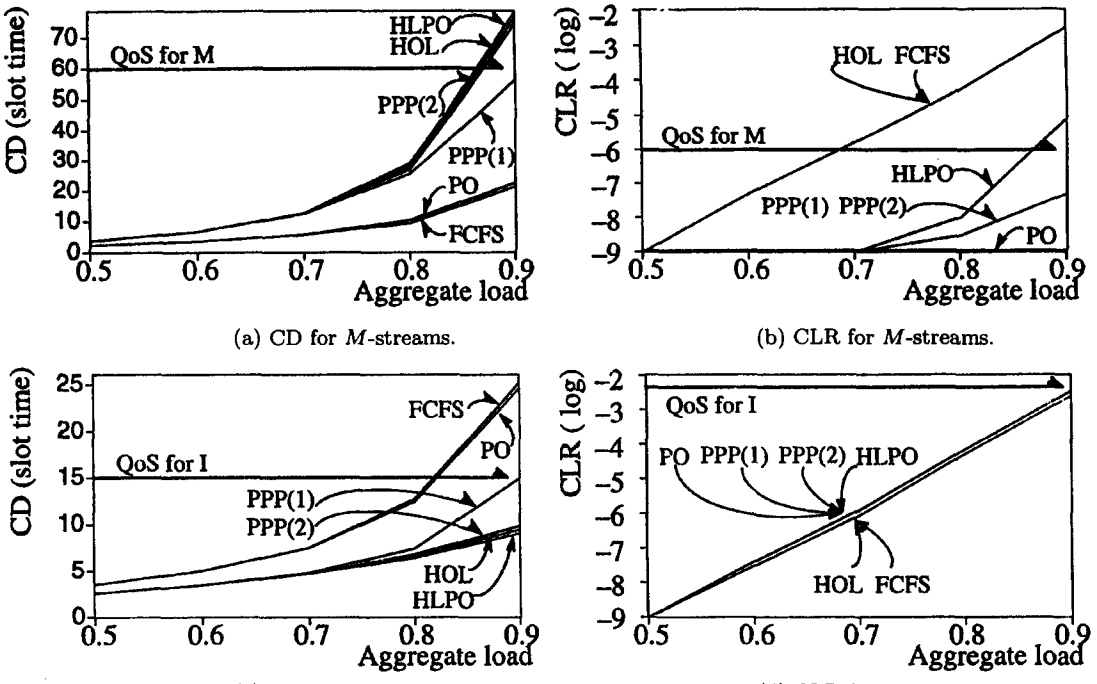

(a) CD for M-streams.

(b) CLR for M-streams.

(c) CD for I-streams.

(d) CLR for I-streams.

Figure 9. CD and CLR based on various disciplines ($N_M = 4$, $K = 100$).

under an aggregate load of 0.9 in Figure 7, an increase in the number of I-streams from 5 (0.1×5) to 6 (0.1×6) results in a decrease in the number of M-streams from 8 (0.05×8) to 6 (0.05×6). This figure depicts that, by employing different Ls and Rs, various quality of the CD and CLR for each traffic class can be achieved. Besides, the greater the L the lower the CD of I-streams, and the lower the R, the lower the CLR of M-streams. These phenomenon agree with the results exhibited in Figures 4 and 6.

The versatility of the PPP discipline is justified in Figures 8 and 9. In Figure 8, the derived CD and CLR of each traffic class based on various disciplines under a given set of ρ and K are depicted. In this figure, HOL gives lowest CD for I-streams but highest CLR for M-streams. PO gives lowest CLR for M-streams but highest CD for I-streams. Since HLPO considers both delay and loss priorities, HLPO greatly improves the CD of I-streams and CLR of M-streams. In addition to considering both delay and loss priorities, PPP provides adjustments of L and R to achieve various quality of CD and CLR for each traffic class. Notice, that the CLR of M-streams based on HLPO is higher than that based on PPP since based on HLPO, the server always serves I-cells as long as there are I-cells in the queue.

The derived CD and CLR of each traffic class based on various disciplines under a given set of N_M and K are drawn in Figure 9. This figure demonstrates that, to support satisfactory QoSs for each traffic class, switch utilization (i.e., aggregate load) is below 0.6 under FCFS or HOL. By employing PO, HLPO, or PPP with $L = 60$ and $R = 30$, switch utilization increases to 0.8. Furthermore, through the use of $L = 20$ and $R = 70$, PPP further improves switch utilization to as high as 0.9. This clearly shows that high switch utilization can be achieved under PPP with proper settings of L and R.

5. CONCLUSIONS

The paper proposed the Precedence with Partial Push-out (PPP) scheduling discipline supporting two delay and two loss priorities in ATM switches. PPP encompasses four widely accepted disciplines, namely FCFS, HOL, PO, and HLPO, by properly setting two thresholds L and R.

For precisely determining L and R retaining demanded QoSs, the paper provided an in-depth queueing analysis based on a discrete-time single-server queueing model with two heterogeneous arrivals, and a simple, algebra-based analysis. The paper showed profound agreement of the analytic results with simulation results. Moreover, we discovered through simulation results that the cell delay of high-delay-priority cells and cell loss ratio of high-loss-priority cells are greatly improved resulting in tolerable performance degradation for cells of other classes. Moreover, the greater the L the lower the cell delay for high-delay-priority cells, and the lower the R the lower the cell loss ratio for high-loss-priority cells. Besides, the cell loss ratio for high-loss-priority cells is greatly improved if L is set to be less than the size of the push-out region. Finally, in addition to the provision of delay and loss QoSs, PPP has also been shown to achieve high switch utilization.

REFERENCES

1. R. Händel, M.N. Huber and S. Schröder, *ATM Networks-Concept, Protocol, Applications*, Second edition, Addison-Wesley, (1993).
2. M.D. Prycker, *Asynchronous Transfer Mode Solution for Broadband ISDN*, Ellis Horwood, (1993).
3. ITU Study Group 13, Traffic control and congestion control in B-ISDN, *Draft Recommendation I.371* (March 1994).
4. J. Daigle, *Queueing Theory for Telecommunications*, Addison-Wesley, (1992).
5. R. Chipalkatti, J.F. Kurose and D. Toesley, Scheduling policies for real-time and nonreal-time traffic in a statistical multiplexer, In *Proc. IEEE INFOCOM'89*, pp. 774–783, (June 1989).
6. S.T. Liang and M.C. Yuang, Performance analysis of earliest-due-date scheduling discipline for ATM switches, in *Proc. IASTED International Conference on Modelling and Simulation* (1996).
7. D.S. Lee and B. Sengupta, Queueing analysis of a threshold based priority scheme for ATM networks, *IEEE/ACM Transactions on Networking* 1 (6) (December 1993).
8. A.Y. Lin and J.A. Silveste, Priority queueing strategies and buffer allocation protocols for traffic control at an ATM integrated broadband switching system, *IEEE J. Select. Areas Commun.* **9** (9), 1524–1536 (December 1991).
9. S. Suri, D. Tipper and G. Meempat, A comparative evaluation of space priority strategies in ATM networks, In *Proc. IEEE INFOCOM'94*, pp. 516–523, (June 1994).
10. P. Yegani, M. Krunz and H. Hughes, Congestion control schemes in prioritized ATM networks, In *Proc. IEEE ICC'94*, pp. 1169–1173, (May 1994).
11. H.J. Chao and I.H. Pekan, Queue management with multiple delay and loss priorities for ATM switches, In *Proc. IEEE ICC'94*, pp. 1184–1189, (May 1994).
12. E.P. Rathgeb, Modeling and performance comparison of policing mechanisms for ATM networks, *IEEE J. Select. Areas Commun.* **9** (3), 325–334 (April 1991).
13. Y. Ohba, M. Murata and H. Miyahara, Analysis of interdeparture processes for bursty traffic in ATM networks, *IEEE J. Select. Areas Commun.* **9** (3), 468–476 (April 1991).
14. J.Y. Hui, Resource allocation for broadband networks, *IEEE J. Select. Areas Commun* **6** (9), 1598–1608 (December 1988).
15. J.M. Hah and M.C. Yuang, Estimation-based call admission control with delay and loss guarantees for ATM networks, In *Proc. IEEE ICC'96*, pp. 787–791, (June 1996).
16. The MATH WORKS Inc., *MATLAB: High-Performance Numeric Computation and Visualization Software*, (August 1992).
17. H. Saito, *Teletraffic Technologies in ATM Networks*, Artech House, (1994).